Front. Chem. China 2008, 3(4): 467–470
DOI 10.1007/s11458-008-0061-9

RESEARCH ARTICLE

Yi LIU, Yitai QIAN

Controllable synthesis of β-$Mn_2V_2O_7$ microtubes and hollow microspheres

Abstract β-$Mn_2V_2O_7$ microtubes with a length of 15–25 μm, 2.5–3.5 μm external diameter, and ~0.4 μm wall thickness, as well as β-$Mn_2V_2O_7$ hollow microspheres with an average outer diameter of 2 μm, were successfully synthesized in a suitable molar ratio of NH_4VO_3 and $MnCO_3$ powders via a hydrothermal process. X-ray powder diffraction (XRD) and field emission scanning electron microscopy (FESEM) were used to characterize the products, and the magnetic susceptibility curve was also measured. In the whole process, the concentration of Mn^{2+} cations derived from $MnCO_3$ dissolution plays a crucial role in the formation of β-$Mn_2V_2O_7$ microtubes and hollow microspheres.

Keywords vanadate, microtubes, hollow microspheres

1 Introduction

Nowadays, much attention has been paid to the preparation and characterization of vanadates with special morphology due to their abnormal behavior and subsequent desirable properties which mainly deal with electrics and magnetics [1,2]. Vanadium oxides and vanadates have activated a new interest as promising electrode materials [3–5]. This may be ascribed to their high-specific capacity and layered crystal structure [6].

Although a number of synthetic means have been developed to prepare vanadates with various sizes and morphologies [7–12], these methods often suffer from the requirements of high temperature, special conditions, tedious procedures and surfactants or templates. Therefore, the development of practical methods for large-scale preparation of vanadates at low cost is still a great challenge for present and future study. β-$Mn_2V_2O_7$, as a typical high-temperature phase of transitional metal divanadates, always adopts the thortveitite ($Sc_2Si_2O_7$) structure [13], which is composed of edge-sharing MnO_6 octahedra, forming $(MnO_3)_n$ layers connected together by V_2O_7 divanadate groups situated on both sides of honeycomb-like cavities. All of the oxygen atoms in the $(MnO_3)_n$ layers are shared with V_2O_7 groups, which adopt a staggered conformation with a linear V-O_b-V moiety [14]. Such layered structures may potentially contribute to the formation of tube-like structures.

Up to now, in the case of the synthesis of β-$Mn_2V_2O_7$, there are only few reports related to the solid-state reaction at high temperature and the wet chemical reactions at low temperature [14]. The synthesis of β-$Mn_2V_2O_7$ microtubes and hollow microspheres have never been reported. Among various conventional synthetic routes, the hydrothermal method, as a wet chemistry method, offers many advantages compared to the usual techniques. One of the main advantages is that the hydrothermal synthetic route can directly obtain high-crystallized powders with uniform grain size-distribution and high purity. The hydrothermal method has also been used for the single-crystal growth of various inorganic materials. In this paper, a hydrothermal process was used to prepare panhydrous $Mn_2V_2O_7$ microtubes and hollow microspheres with a large-scale treatment of bulky NH_4VO_3 and $MnCO_3$ powders without using any template and surfactants.

Received March 12

Yi LIU
Department of Chemistry, University of Science and Technology of China, Hefei 230026, China

Yi LIU (✉), Yitai QIAN
Department of Chemistry, Zaozhuang University, Zaozhuang 277160, China
E-mail: liuyi67@ustc.edu.cn

2 Experimental

All reagents used in the experiments were of 99.9% purity (Shanghai Chemical Reagents Co.) and were used without further purification. In a typical procedure, 2 mmol of the ammonium metavanadate (NH_4VO_3) was dissolved in 20 mL of distilled water at 90°C under vigorous stirring,

and then 1 mmol manganese carbonate ($MnCO_3$) was added to the NH_4VO_3 solution to form a heterogeneous solution, which was transferred into a 50 mL stainless steel autoclave with a Teflon-liner. The autoclave was filled with distilled water up to 80% of its capacity. After that, one experiment situation was that the autoclave was directly heated to 180°C for 16 h. In the second experiment, the autoclave was first heated to 90°C for 8 h, and then maintained at 180°C for 16 h. Finally, the autoclave was cooled to room temperature naturally. The products were carefully collected and washed with distilled water and absolute ethanol several times to remove the residues, and then dried in a vacuum at 80°C for 1 h. The as-prepared products direct heated to 180°C for 16 h were β-$Mn_2V_2O_7$ microtubes. The products first aged at 90°C for 8 h and then maintained at 180°C for 16 h were β-$Mn_2V_2O_7$ hollow microspheres.

X-ray powder diffraction (XRD) pattern was taken on a Japan Rigaku D/max-γA X-ray diffractometer equipped with graphite monochromatized Cu Kα radiation ($\lambda = 0.15418$ nm). Field emission scanning electron microscopy (FESEM) images were taken with a JEOL-6700F scanning electronic microanalyzer. Magnetic properties were measured on a MPMS XL-7 SQUID magnetometer.

3 Results and discussion

Figure 1 shows the XRD patterns of the as-prepared β-$Mn_2V_2O_7$ hollow microspheres and the tubular β-$Mn_2V_2O_7$ crystals, respectively. Figure 1(a) is the XRD pattern of the as-prepared β-$Mn_2V_2O_7$ microtubes. The peaks are in agreement with monoclinic $Mn_2V_2O_7$ [S.G.: C2/m (12)]. Figure 1b is the XRD pattern of the monoclinic $Mn_2V_2O_7$ hollow microspheres. All diffraction peaks could be indexed as a monoclinic structure

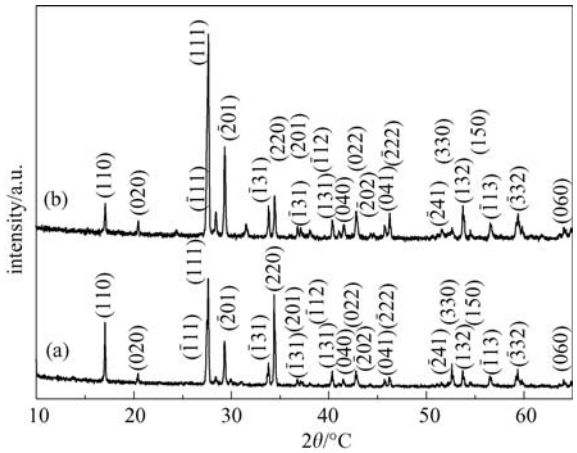

Fig. 1 Typical XRD patterns of the as-prepared $Mn_2V_2O_7$ samples: (a) $Mn_2V_2O_7$ microtubes, (b) $Mn_2V_2O_7$ hollow microspheres

$Mn_2V_2O_7$ with cell constants $a = 6.70$Å, $b = 8.72$Å, $c = 4.96$Å, $\beta = 104.2°$, which are in agreement with the reported value (JCPDS No. 22-0436, $a = 6.71$Å, $b = 8.726$Å, $c = 4.97$Å, $\beta = 103.57°$), and no impurity phases were found in the XRD patterns.

The field emission scanning electron microscopy (FESEM) images of β-$Mn_2V_2O_7$ microtubes and hollow microspheres are shown in Fig 2. Figure 2(a) and (b) are the low and high magnification FESEM images of β-$Mn_2V_2O_7$ microtubes, respectively. These images show that the final products of β-$Mn_2V_2O_7$ consisted of a large number of microtubes with an external diameter of 2.5–3.5 μm, wall thickness of ~0.4 μm and lengths up to 15–25 μm. Figure 2(c) and (d) are the low and high magnification FESEM images of β-$Mn_2V_2O_7$ hollow microspheres with average outer diameter of 2 μm, respectively.

An investigation of the magnetic susceptibility was undertaken in order to determine if $Mn_2V_2O_7$ possesses low-dimensional magnetic properties. The magnetic susceptibility for the representative $Mn_2V_2O_7$ microtubes was tentatively measured between 2 K–50 K. Figure 3 is a plot of the magnetic susceptibility for the representative $Mn_2V_2O_7$ microtubes between 2 K–50 K. The results exhibit that a paramagnetic–antiferromagnetic transition occurs at $T_N = 18.2(5)$ K, which accords with the previous result of $T_N = 16.0(5)$ K [14], confirming that the synthesized product is β-$Mn_2V_2O_7$.

In this experiment, the formation of β-$Mn_2V_2O_7$ microtubes and hollow microspheres can be described by the following reactions:

$$MnCo_3 \longrightarrow Mn^{2+} + CO_3^{2-} \quad (1)$$

$$2Mn^{2+} + 2CO_3^{2-} + 2NH_4VO_3 \longrightarrow Mn_2V_2O_7 + (NH_4)_2CO_3 + CO_2 \quad (2)$$

The possible formation mechanism for the β-$Mn_2V_2O_7$ microtubes and hollow microspheres is discussed as follows. The initial concentration of Mn^{2+} cations derived from $MnCO_3$ dissolution has a significant effect on the morphologies of β-$Mn_2V_2O_7$. When hydrothermal temperature is directly elevated to 180°C, the initial concentration of Mn^{2+} in solution is lower owing to insufficiently dissolved $MnCO_3$. As a result, the Mn^{2+} cations can selectively insert the layered-structure of ammonium metavanadate, which favors the one-dimensional structure growth, so that β-$Mn_2V_2O_7$ forms microtube-like structure. This is consistent with the literature report [15]. While hydrothermal temperature is first elevated to 90°C and aged for 8 h, and then elevated to 180°C, the initial concentration of Mn^{2+} cations derived from $MnCO_3$ dissolution increases. Thus, the Mn^{2+} cations can randomly insert the layered-structure of vanadium oxides, which favors β-$Mn_2V_2O_7$ to grow into hollow

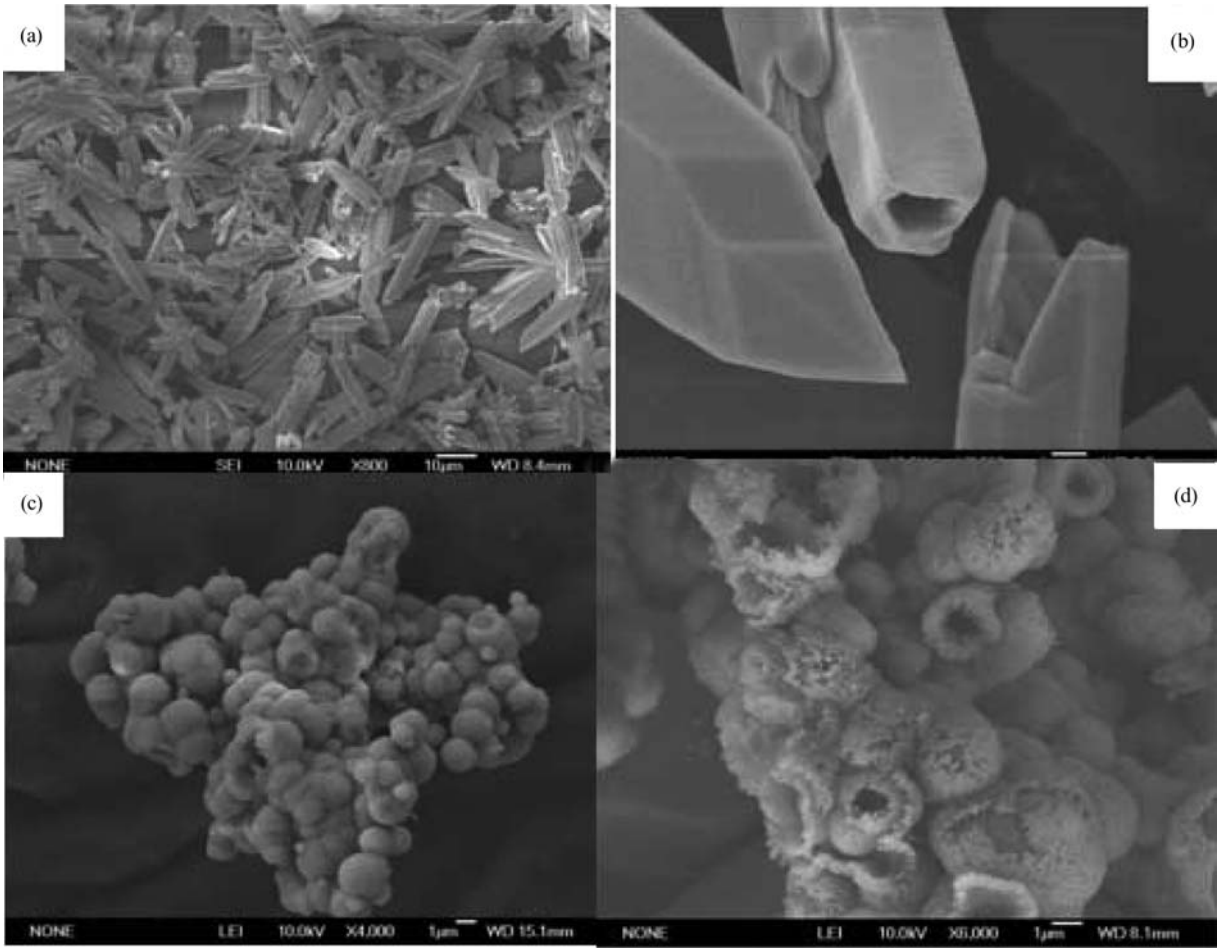

Fig. 2 The FESEM images of $Mn_2V_2O_7$ microtubes and hollow microspheres: (a) and (c) low magnification FESEM images, (b) and (d) high magnification images

microsphere-like structures. Moreover, the presence of CO_2 as by-product may contribute to the formation of hollow structures of β-$Mn_2V_2O_7$.

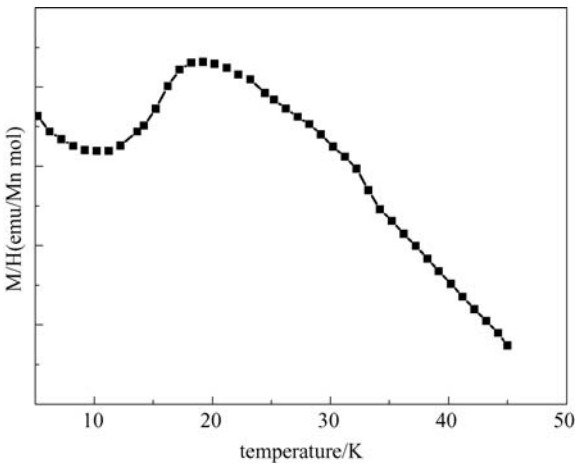

Fig. 3 The magnetic susceptibility for the representative $Mn_2V_2O_7$ microtubes measured between 2–50 K.

Acknowledgements This work was supported by the National Natural Science Foundation of China and the National Basic Research Program of China (No. 2005CB623601).

References

1. Fey G T-K, Huang D L. Synthesis, characterization and cell performance of inverse spinel electrode materials for lithium secondary batteries. Electrochimica Acta, 1999, 45: 295–314
2. Prokofieva AV, Kremerb R K, Assmu W. Crystal growth and magnetic properties of α-CuV_2O_6. J Cryst Growth, 2001, 231: 498–505
3. Baudrin E, Laruelle S, Denis S. et al Synthesis and electrochemical properties of cobalt vanadates vs. lithium. Solid State Ionics, 1999, 123: 139–153
4. Kim S S, Ikuta H, Wakihara M. Synthesis and characterization of MnV_2O_6 as a high capacity anode material for a lithium secondary battery, Solid State Ionics, 2001, 139: 57–65
5. Hara D, Ikuta H, Uchimoto Y et al. Electrochemical properties of manganese vanadium molybdenum oxide as the anode for Li secondary batteries. J Mater Chem, 2002, 12: 2507–2512
6. Inagaki M, Morishita T, Hirano M, et al. Synthesis of MnV_2O_6 under autogenous hydrothermal conditions and its anodic performance, Solid State Ionics, 2003, 156: 275–282

7. Tian H J, Wachs I E, Briand L E. Comparison of UV and visible raman spectroscopy of bulk metal molybdate and metal vanadate catalysts. J Phys Chem B, 2005, 109: 23491–23499
8. Yahia H B, Gaudin E, Darriet J et al. Synthesis, Crystal structure, magnetic properties, and electronic structure of the new ternary vanadate $CuMnVO_4$. Inorg Chem, 2005, 44: 3087–3093
9. Niederberger M, Muhr H J, Krumeich F, et al. Low-cost synthesis of vanadium oxide nanotubes via two novel non-alkoxide routes. Chem Mater, 2000, 7: 1995–2000
10. Kong L F, Shao M W, Xie Q, et al. Hydrothermal growth of single-crystal $CaV_6O_{16}\cdot 3H_2O$ nanoribbons. J Cryst Growth, 2004, 260: 435–439
11. Yu J G, Yu Jimmy C, Ho W K et al. J Am Chem Soc, 2004, 126: 3422–3423
12. Liu Y, Zhang Y G, Hu Y H et al. Hydrothermal synthesis of single-crystal beta-$AgVO_3$ nanowires and ribbon-like nanowires. Chem Lett, 2005, 34: 146–147
13. Zachariasen W H. The structure of thortveitite $Sc_2Si_2O_7$. Z Kristallogr, 1930, 73: 1–6
14. Liao J H, Leroux F, Payen C et al. Synthesis, structures, magnetic properties, and phase transition of manganese(II) divanadate: $Mn_2V_2O_7$. J Solid State Chem, 1996, 121: 214–224
15. Liu Z P, Li S, Yang Y et al. Shape-controlled synthesis and growth mechanism of one-dimensional nanostructures of trigonal tellurium. New J Chem, 2003, 27: 1748–1752